

# Fourier Analysis on Regular and Irregular Astigmatism of Anterior and Posterior Corneal Surfaces in Fuchs Endothelial Corneal Dystrophy



YOSHINORI OIE, YUICHI YASUKURA, NOZOMI NISHIDA, SHIZUKA KOH, RYO KAWASAKI, NAOYUKI MAEDA, VISHAL JHANJI, AND KOHJI NISHIDA

- **PURPOSE:** To conduct Fourier analysis on regular and irregular astigmatism of the anterior and posterior corneal surfaces using anterior segment optical coherence tomography in patients with Fuchs endothelial corneal dystrophy (FECD)
- **DESIGN:** Observational case series.
- **METHODS:** This study included 75 eyes of 43 FECD patients and 34 eyes of 34 healthy subjects in Osaka University Hospital. Corneal dioptric data from the central 6-mm zone of the anterior and posterior corneal surface were expanded into spherical, regular astigmatism, asymmetry, and higher-order irregularity components using Fourier analysis. We analyzed the association between each component and modified Krachmer grade.
- **RESULTS:** There were significant differences in regular astigmatism, asymmetry, and higher-order irregularity components of the anterior corneal surface, and spherical, regular astigmatism, asymmetry, and higher-order irregularity components of the posterior corneal surface among modified Krachmer grades ( $P = .036, <.001, <.001, <.001, <.001, <.001, <.001$ , respectively). Asymmetry component of the anterior and posterior corneal surfaces gradually increased with FECD progression. Higher-order irregularity components of the anterior and posterior corneal surfaces drastically increased in Grade 6. Many eyes had an axis of  $0^\circ$ - $180^\circ$  for the asymmetry component of the anterior surface and  $180^\circ$ - $360^\circ$  for that of the posterior surface.
- **CONCLUSION:** Patients with severe FECD had a larger amount of asymmetry and higher-order irregularity components of the anterior and posterior corneal surfaces. Patients with FECD up to Grade 5 were characterized by anterior and posterior flattening in the inferior cornea, and those with Grade 6 showed irregularity in the ante-

rior and posterior corneal surfaces. (*Am J Ophthalmol* 2021;223:33–41. © 2020 Elsevier Inc. All rights reserved.)

**F**UCHS ENDOTHELIAL CORNEAL DYSTROPHY (FECD) IS a bilateral disorder characterized by abnormal deposition of the extracellular matrix. The clinical features include corneal guttae, thickening of Descemet membrane, and subsequent corneal endothelial pump dysfunction.<sup>1</sup> The corneal guttae are dominant in the central cornea, and the inferotemporal endothelium is damaged more severely among peripheral zones.<sup>2</sup> Some FECD patients complain of visual deterioration, even if they do not have apparent corneal stromal or epithelial edema under slit-lamp examination. Intraocular forward light scatter impairs the quality of vision, and corneal guttae associated with FECD cause intraocular light scatter and glare, which can have debilitating effects on the quality of vision despite an absence of edema.<sup>3,4</sup>

Anterior segment optical coherence tomography (AS-OCT) provides no-contact, rapid in vivo imaging of ocular structures, and has become a key examination of the anterior segment of the eye.<sup>5–7</sup> There are 2 types of Fourier domain AS-OCT: spectral domain and swept-source. Swept-source AS-OCT has the advantages of a wide observation range and high penetration in eyes with corneal opacification compared with spectral domain AS-OCT.<sup>8</sup> Therefore, it enabled us to evaluate not only the anterior surface but also the posterior surface of the cornea and stromal thickness profile even in eyes with corneal opacification.

Fourier series harmonic analysis is very useful to quantify spherical power, regular astigmatism, and irregular astigmatism, including asymmetry component and higher-order irregularity.<sup>9–12</sup> It has been successfully used to evaluate corneal shape in eyes with corneal diseases or following ocular surgery.<sup>11,13–15</sup>

Although it was reported that corneal guttae occurred asymmetrically, and were predominant in the inferior temporal area,<sup>2,16</sup> subsequent morphologic asymmetrical and irregular changes of both the anterior and posterior surfaces of the cornea have not been elucidated. Thus, Fourier analysis was conducted on regular and irregular astigmatism of

AJO.com

Supplemental Material available at [AJO.com](https://www.ajocom.com).

Accepted for publication Sep 23, 2020.

From the Department of Ophthalmology, Osaka University Graduate School of Medicine (Y.O., Y.Y., N.N., S.K., R.K., N.M., K.N.), Suita, Osaka, Japan; and Department of Ophthalmology, University of Pittsburgh School of Medicine (V.J.), Pittsburgh, Pennsylvania, USA.

Inquiries to Yoshinori Oie, Department of Ophthalmology, Osaka University Graduate School of Medicine, Yamadaoka 2-2, Osaka 565-0871, Japan; e-mail: [yoie@ophthal.med.osaka-u.ac.jp](mailto:yoie@ophthal.med.osaka-u.ac.jp)

the anterior and posterior corneal surface using AS-OCT in patients with FECD to clarify the point. The association between Fourier components and visual function was also analyzed.

## METHODS

THE MEDICAL CHARTS OF PATIENTS WITH FECD AND healthy subjects at the Department of Ophthalmology at Osaka University Hospital were retrospectively reviewed. Cornea specialists diagnosed all cases of FECD based on the presence of longstanding bilateral corneal guttae or a beaten metal appearance without other causative abnormalities such as surgery or inflammation.<sup>17</sup> The severity of FECD was determined by modified Krachmer grade.<sup>18,19</sup> Patients with other corneal diseases or previous intraocular surgery were excluded. The Institutional Review Board of Osaka University Hospital approved this observational study and waived the requirement for informed consent because of the retrospective nature of the study. The research adhered to the tenets of the Declaration of Helsinki.

Central corneal thickness (CCT) and corneal dioptric data from the central 3-mm and 6-mm zone of the anterior and posterior corneal surface were measured using the SS-1000 (TOMEY, Nagoya, Japan). Corneal dioptric data were expanded into spherical, regular astigmatism, asymmetry, and higher-order irregularity components using Fourier analysis. This swept-source AS-OCT achieves 10  $\mu\text{m}$  axial and 30  $\mu\text{m}$  lateral high-resolution imaging and high-speed scanning of 30,000 A-scans per second.

The association between severity of modified Krachmer grade or CCT and each component was analyzed. The subjects were divided into 5 categories based on the CCT: 549  $\mu\text{m}$  or thinner, 550-599  $\mu\text{m}$ , 600-649  $\mu\text{m}$ , 650-699  $\mu\text{m}$ , 700  $\mu\text{m}$  or thicker.

The association between corrected distance visual acuity (CDVA) and each Fourier component was measured in a subgroup analysis. Eyes with nuclear cataract Grade 2 or lower were included to minimize the effect of lens opacity on visual acuity.<sup>20</sup> The CDVA was expressed in logarithm of the minimum angle of resolution (logMAR) units after the decimal visual acuity was measured. Spearman rank correlation coefficient was calculated for the association.

We understand that there might be concern regarding the use of data from both eyes, which can potentially result in a high correlation between the right and left eyes, thereby biasing the result. This is especially true when characteristics of personwise information such as age and gender are used twice in patients with FECD. Therefore, we did not use personwise information, and used only eyewise data derived within the same eye, namely, spherical, regular astigmatism, asymmetry, and higher-order irregularity components by Fourier analysis. There is a possibility that the association between parameters within

TABLE. Patients Characteristics

Modified Krachmer Grade	Control		FECD					Total
	0	1	2	3	4	5	6	
Guttae/edema	No	1-12 Nonconfluent	>12 Nonconfluent	1-2 mm Confluent	2-5 mm Confluent	>5 mm Confluent	>5 mm Confluent with edema	75
Number of eyes (eyes)	34	4	13	14	29	11	4	75
Age, y								
Mean $\pm$ SD	69.4 $\pm$ 12.1	57.8 $\pm$ 10.3	58.1 $\pm$ 14.8	62.4 $\pm$ 15.1	67.7 $\pm$ 9.0	69.3 $\pm$ 8.3	64.3 $\pm$ 12.9	64.6 $\pm$ 12.4
Range	19-87	48-75	33-84	33-80	44-80	55-86	49-79	33-86
Females (eyes), %	58.8	100	76.9	64.3	75.9	63.6	75	74.7
CCT, $\mu\text{m}$	541.4 $\pm$ 29.0	499 $\pm$ 4.9	563.6 $\pm$ 41.9	566.6 $\pm$ 41.8	593.1 $\pm$ 43.6	624.0 $\pm$ 32.1	700.8 $\pm$ 89.3	588.3 $\pm$ 59.0

CCT = central corneal thickness, FECD = Fuchs endothelial corneal dystrophy.

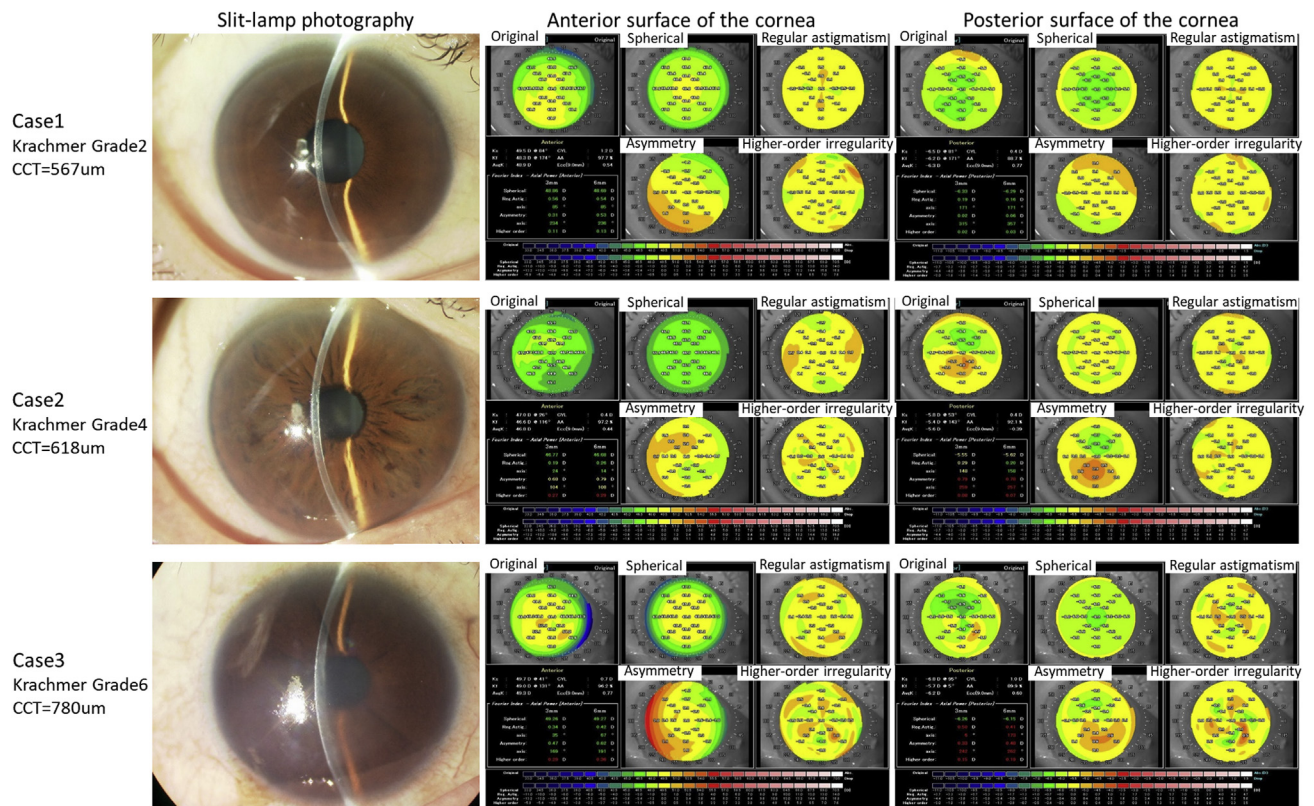


FIGURE 1. Representative cases with Fourier analysis for anterior and posterior surfaces of the cornea using AS-OCT. Slit-lamp photography and Fourier analysis for the anterior and posterior surfaces of the cornea are shown for each grade.

individual eyes can be associated differently in its magnitude. We consider that the association between eye-specific parameters within a person (ie, the right eye and the left eye of patient A) is not hugely different between persons (ie, the right eye of patient B and the right eye of the patient C). We assume that the interperson heterogeneity in association between eye-specific parameters are minimal and adopted both eyes' data to be included. To confirm the validity of our assumption and findings, we added an analysis using one eye from patients with FECD and normal subjects. The methods are described in the [Supplemental Material](#).

Kruskal-Wallis test was used to compare differences among grades. Steel-Dwass analysis was used to compare parameters for each pair. All statistical analyses were performed using JMP version 14.0.0 (SAS Institute Inc, Tokyo, Japan);  $P$  values  $<.05$  were defined as statistically significant. All statistical analyses were conducted with the guidance of a biostatistician (RK).

## RESULTS

SEVENTY-FIVE EYES OF 43 FECD PATIENTS AND 34 EYES OF 34 healthy subjects were enrolled in the current study. Char-

acteristics of the subjects are shown in [Table](#). Representative cases are shown in [Figure 1](#). Case 1 was mild, with modified Krachmer Grade 2 and CCT of  $567\ \mu\text{m}$ . The anterior surface had mild regular astigmatism with the rule, and the posterior surface had mild astigmatism against the rule. Asymmetry and higher-order irregularity components were very small. Tomographic abnormalities in this case were thought to be minimal. Case 2 was moderate, with Grade 4 and CCT of  $618\ \mu\text{m}$ . The anterior surface had steeper power in the superior cornea and flatter in the inferior cornea. Thus, the asymmetry component was  $0.68\text{D}$  with an axis of  $104^\circ$  at  $3\ \text{mm}$  and  $0.79\text{D}$  with an axis of  $108^\circ$  at  $6\ \text{mm}$ . Higher-order irregularity component was  $0.27\text{D}$  at  $3\ \text{mm}$  and  $0.29\text{D}$  at  $6\ \text{mm}$ . Posterior surface map revealed a steeper area in the superior cornea and a flatter one in the inferior. The asymmetry component was  $0.79\text{D}$  with an axis of  $259^\circ$  at  $3\ \text{mm}$  and  $0.78\text{D}$  with an axis of  $257^\circ$  at  $6\ \text{mm}$ . The high-order irregularity component was  $0.08\text{D}$  at  $3\ \text{mm}$  and  $0.07\text{D}$  at  $6\ \text{mm}$ . Case 3 was severe, with Grade 6 and CCT of  $780\ \mu\text{m}$ . The anterior surface showed a mild steepening pattern, presumably because of epithelial edema. Higher-order irregularity component was remarkably increased to  $0.29\text{D}$  at  $3\ \text{mm}$  and to  $0.36\text{D}$  at  $6\ \text{mm}$ . The posterior surface also indicated asymmetric pattern with significant inferior flattening. Therefore, it increased the asymmetry component of  $0.33\text{D}$  with an

## Anterior surface of the cornea

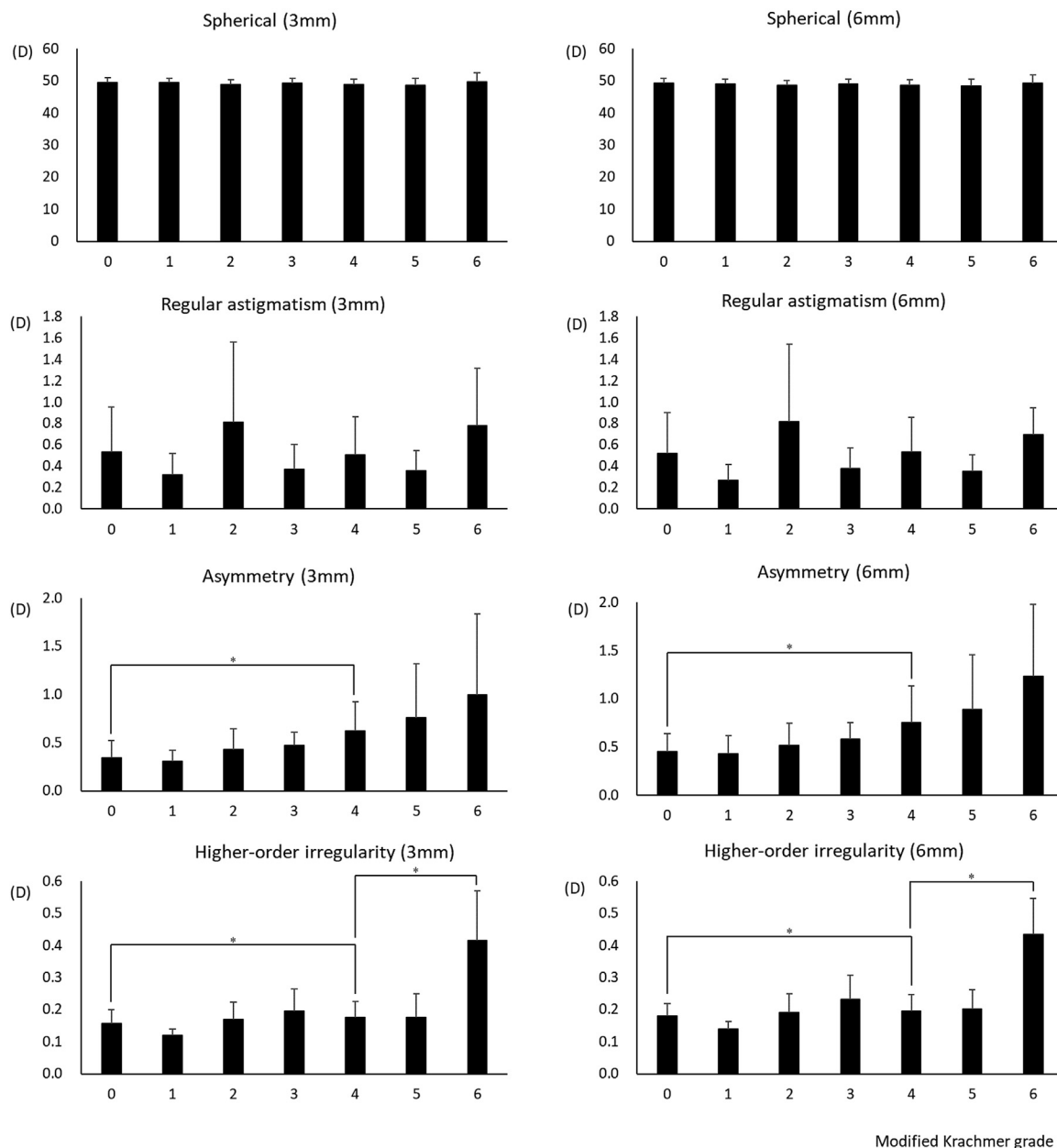


FIGURE 2. Fourier indices of the anterior surface of the cornea according to modified Krachmer grade. \* $P < .05$  by Steel-Dwass analysis.

axis of  $242^\circ$  at 3 mm, 0.48D with an axis of  $262^\circ$  at 6 mm, and higher-order irregularity component 0.15D at 3 mm and 0.19D at 6 mm.

Quantitative evaluation on spherical power, regular astigmatism, asymmetry, and higher-order irregularity components for the anterior surface of the cornea was shown according to a modified Krachmer grade in Figure 2. There were significant differences among grades in regular astigmatism at 6 mm, asymmetry component at 3 and 6 mm, and higher-order irregular component at 3

and 6 mm ( $P = .036, < .001, < .001, < .001, < .001$ ). There were no significant differences among grades in terms of spherical power and regular astigmatism at 3 mm and spherical power at 6 mm ( $P = .66, .17, .65$ , respectively). The asymmetry component of the anterior corneal surface gradually increased with FECD progression. Higher-order irregularity component of the anterior corneal surface increased in Grade 6.

Quantitative evaluation on Fourier analysis for the posterior surface of the cornea was also shown according to

## Posterior surface of the cornea

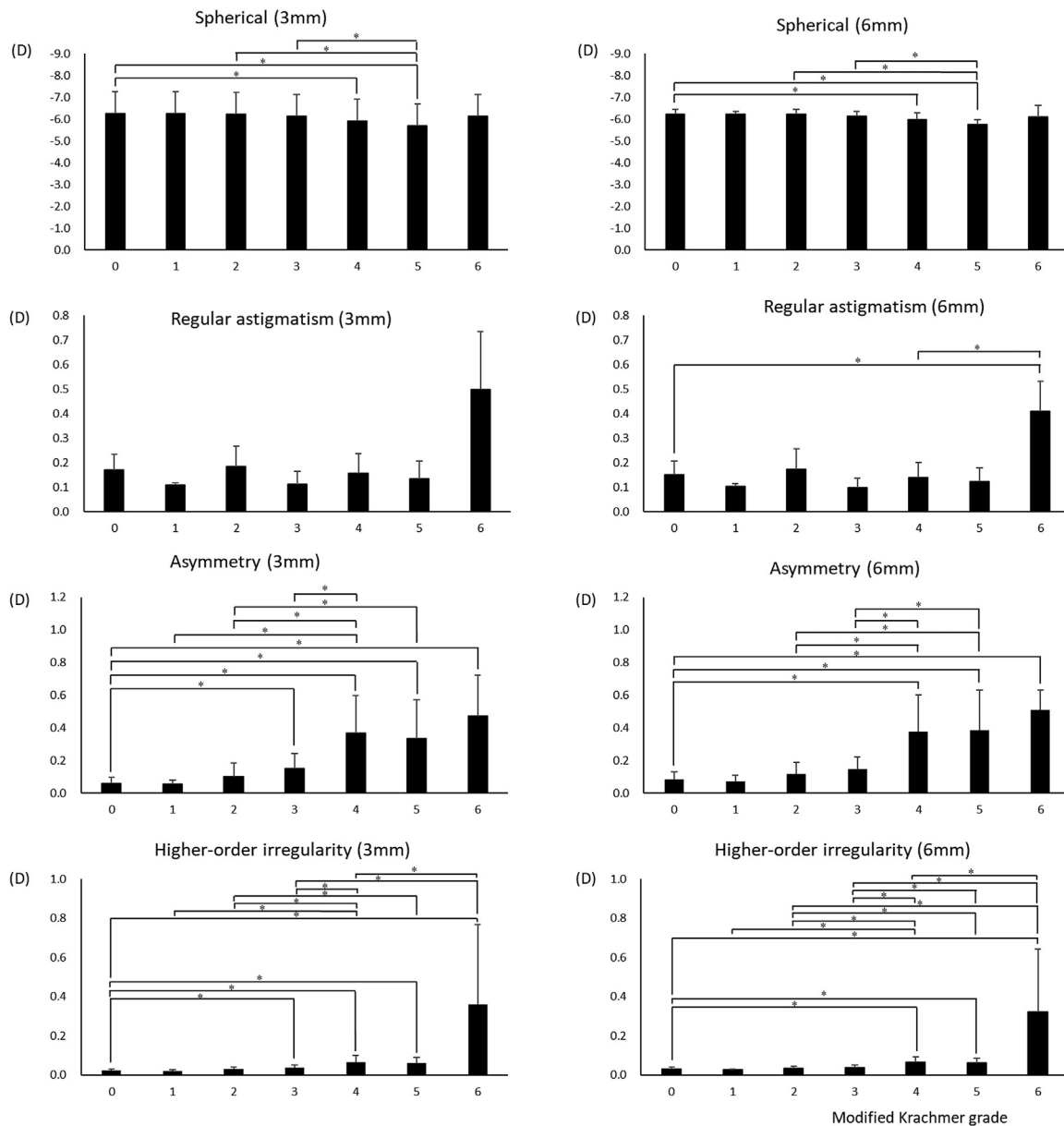
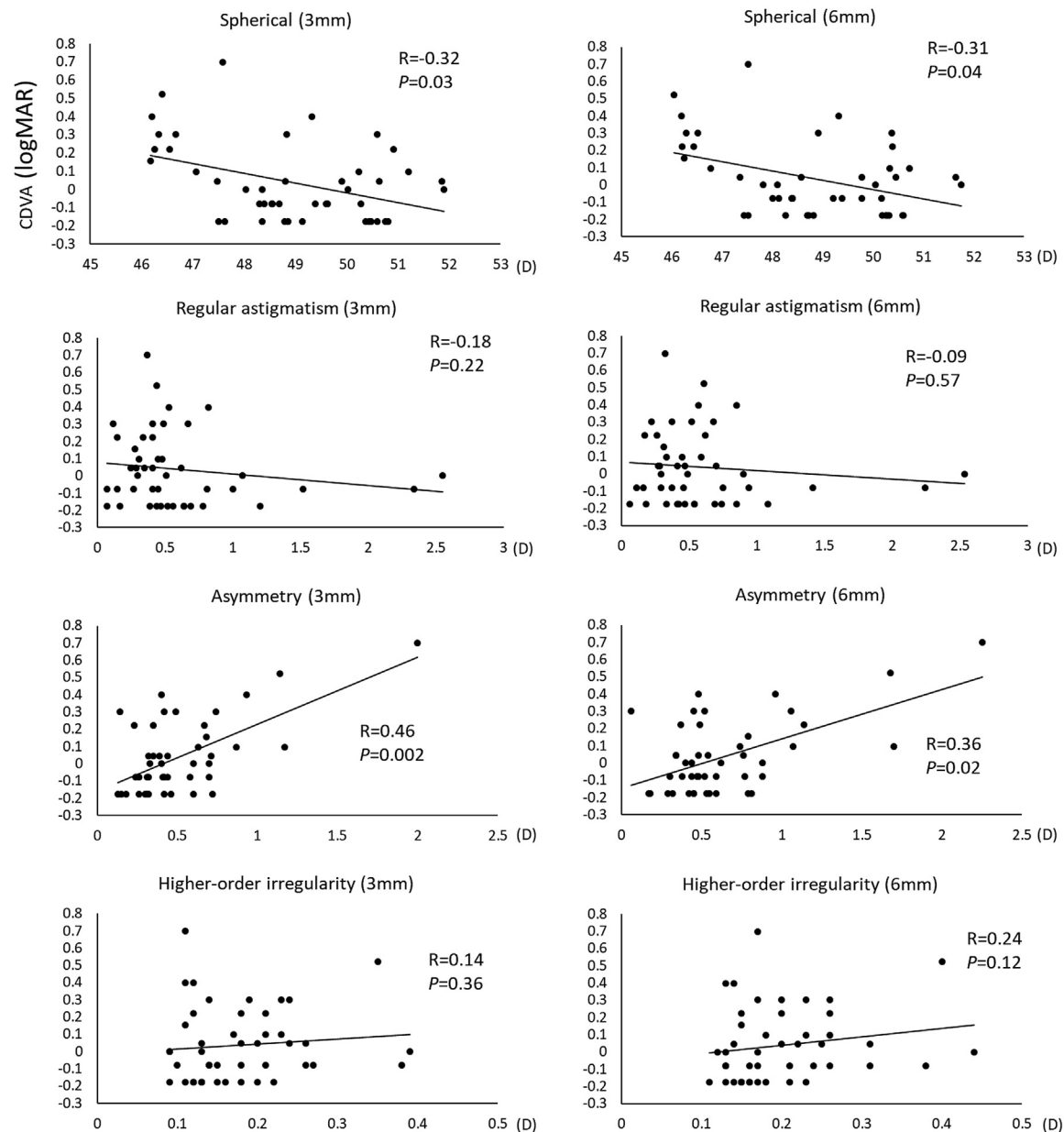


FIGURE 3. Fourier indices of the posterior surface of the cornea according to modified Krachmer grade. \* $P < .05$  by Steel-Dwass analysis.

modified Krachmer grade in Figure 3. There were significant differences among grades in spherical power, regular astigmatism, asymmetry component, and higher-order irregular component at both 3 and 6 mm ( $P = .001, < .001, .003, .005, < .001, < .001, < .001, < .001$ , respectively). Spherical power of the posterior corneal surface gradually decreased up to Grade 5. The asymmetry component of the posterior surface gradually increased with the severity of FECD. Drastic increase of higher-order irregularity component of the posterior surface was found in Grade 6.

A similar evaluation of the anterior and posterior surfaces of the cornea was conducted for CCT, and the results are shown in Supplemental Figures S1 and S2. For the anterior surface, there were significant differences among grades in spherical power, asymmetry component, and higher-order irregular component at both 3 and 6 mm ( $P = .005, .005, < .001, .001, .006, \text{ and } .01$ , respectively). There were no significant differences in regular astigmatism at 3 and 6 mm ( $P = .73$  and  $.49$ , respectively). For the posterior surface, there were also significant differences in spherical power, asymmetry components, and higher-

## Anterior surface of the cornea



**FIGURE 4.** Association between CDVA and Fourier components in the anterior surface of the cornea. There were significant associations between CDVA and spherical power and asymmetry component at both 3 and 6 mm.

order irregular components at both 3 and 6 mm ( $<.001$  for all). There were no significant differences in regular astigmatism at 3- and 6 mm ( $P = .15$  and  $.15$ , respectively).

Supplemental Figure S3 shows scatterplots of regular astigmatism of the anterior and posterior surface at 3 and 6 mm. Most of the eyes have the axis of  $0^\circ$  or  $90^\circ$ , astigmatism with the rule or against the rule in the anterior surface. On the other hand, most of them had an axis of  $0^\circ$ , astigmatism against the rule in the posterior surface despite the astigmatism with the rule or against the rule at the anterior surface. Double-angle scatter plots of the asymmetry

component of the anterior and posterior surfaces at 3 and 6 mm are shown in Supplemental Figure S4. Many eyes had the axis of  $0^\circ$ - $180^\circ$  for the anterior surface and  $180^\circ$ - $360^\circ$  for the posterior surface. Therefore, the axis of the anterior surface was often opposite that of the posterior surface.

Subgroup analysis for visual acuity was conducted with 45 eyes of 26 FECD patients complicated with nuclear cataract of 2 or less. Four eyes were graded as 1, ten as 2, eight as 3, fourteen as 4, seven as 5, and two as 6 by the modified Krachmer grade. The association between CDVA and

## Posterior surface of the cornea

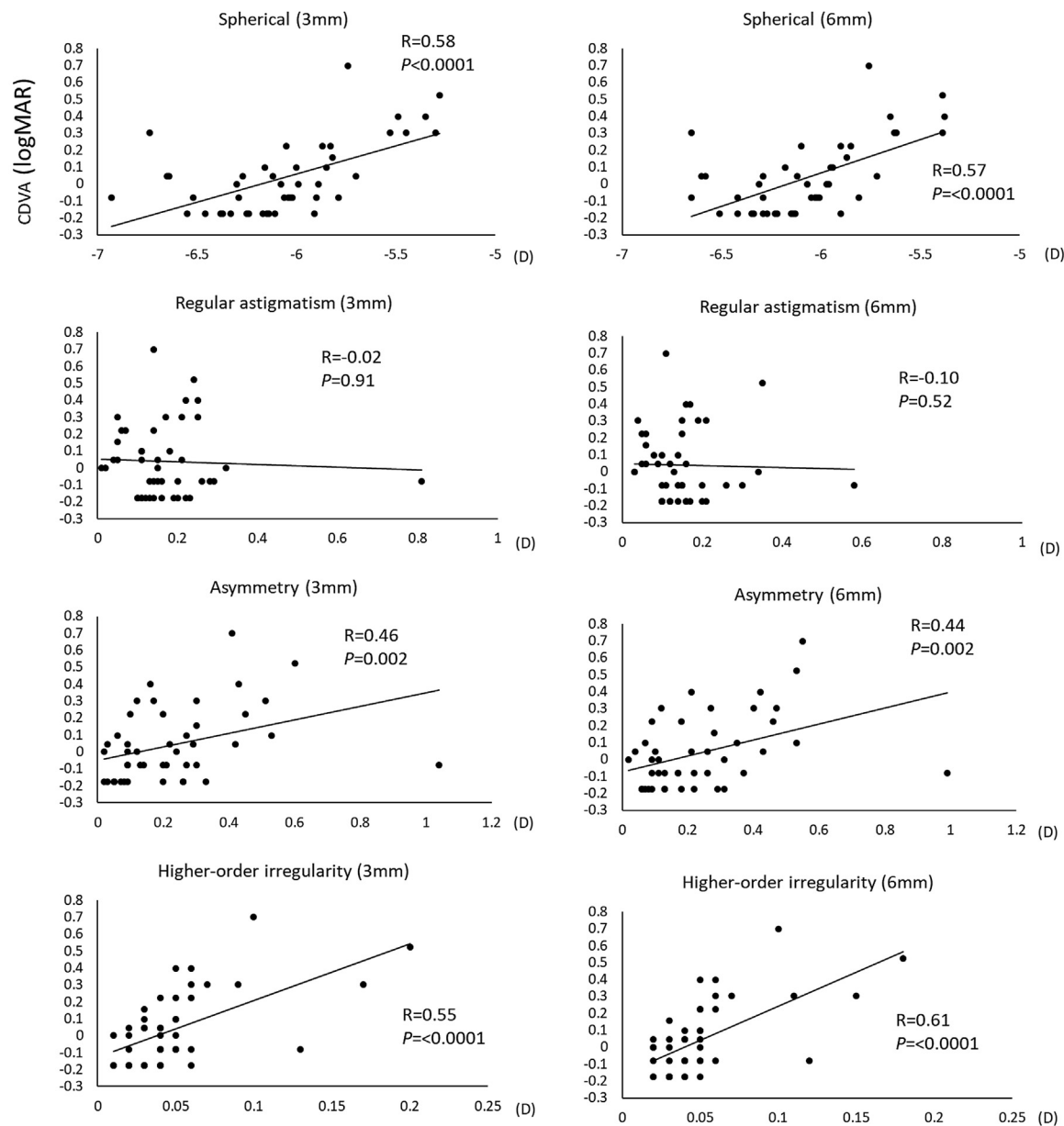


FIGURE 5. Association between CDVA and Fourier components in the posterior surface of the cornea. There were significant associations between CDVA and spherical power, asymmetry, and higher-order irregularity components at both 3 mm and 6 mm.

each Fourier component of the anterior and posterior cornea surface is shown in Figures 4 and 5.

For the anterior surface, there were significant associations between CDVA and spherical power, asymmetry component at both 3 and 6 mm ( $R = -0.32$ ,  $P = .03$ ;  $R = 0.46$ ,  $P = .002$ ;  $R = -0.31$ ,  $P = .04$ ;  $R = 0.36$ ,  $P = .02$ , respectively). There were no significant associations between CDVA and regular astigmatism, higher-order irregularity at 3 and 6 mm ( $R = -0.18$ ,  $P = .22$ ;  $R = 0.14$ ,  $P = .36$ ;  $R = -0.09$ ,  $P = .57$ ;  $R = 0.24$ ,  $P = .12$ , respectively).

For the posterior surface, there were significant associations between CDVA and spherical power, asymmetry, higher-order irregularity component at both 3 and 6 mm ( $R = 0.58$ ,  $P < .0001$ ;  $R = 0.46$ ,  $P = .002$ ;  $R = 0.55$ ,  $P < .0001$ ;  $R = 0.57$ ,  $P < .0001$ ,  $R = 0.44$ ,  $P = .002$ ;  $R = 0.61$ ,  $P < .0001$ , respectively). There were no significant associations between CDVA and regular astigmatism at 3 and 6 mm ( $R = -0.02$ ,  $P = .91$ ;  $R = -0.10$ ,  $P = .52$ , respectively).

The results of one eye from patients with FECD and normal subjects are shown in the supplemental file.

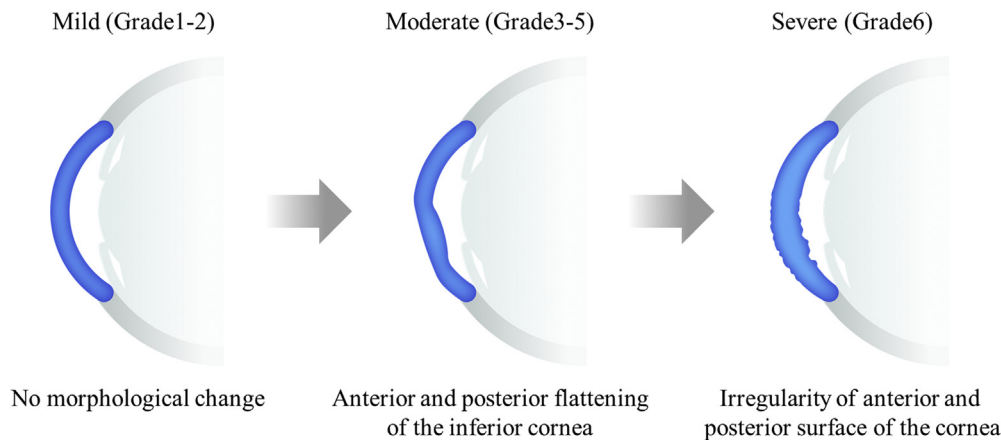


**FIGURE 6.** Illustrations showing corneal optical change with Fuchs endothelial corneal dystrophy (FECD) progression. Corneal optical change was shown using a schema with disease progression.

Overall, the results of one eye were very similar to those of both eyes.

## DISCUSSION AND CONCLUSION

FOR THE ANTERIOR SURFACE OF THE CORNEA, WE DEMONSTRATED that severe FECD patients had a larger amount of asymmetry and higher-order irregularity components using Fourier analysis. In fact, the asymmetry component gradually increased with FECD progression, and the higher-order irregularity component abruptly increased with the onset of corneal edema. For the posterior surface of the cornea, we found that subjects with a severe grade had flatter spherical component, higher asymmetry, and higher-order irregularity components. Flattening of the posterior surface gradually increased up to the onset of corneal edema represented up to Krachmer Grade 6. Asymmetry component in the posterior surface steadily increased with progression. However, higher-order irregularity components suddenly accrued with the onset of edema. Therefore, tomographic and optical change in patients with FECD before the development of edema seemed to be different after that point.

Wacker and associates reported that anterior and posterior corneal higher-order aberrations are higher than normal eyes even in early stages of FECD measured with Scheimpflug imaging.<sup>21</sup> They also reported that posterior toricity is abnormal in advanced FECD because of relatively greater horizontal than vertical corneal thickening, and posterior corneal power decreases in moderate and advanced FECD.<sup>22</sup> These results conducted by the Scheimpflug rotating camera were generally similar with those in the current study assessed by AS-OCT although Fourier analysis was not used in the past study. Nowinska and associates reported there was no posterior elevation mirror symmetry with the greatest degree of irregularity

(Nowinska A et al. IOVS 2018; 59: ARVO E-Abstract 5738). Although the results with higher-order irregularity were similar to those in the current study, the results with asymmetry components did not coincide. Their results are very interesting and will provide a good comparison group for our results.

Corneal tomographic changes with FECD progression suggested by the current study are schematically described in Figure 6. Mild cases with nonconfluent guttae have no tomographic change because the endothelial pump function is supposed to be within normal range. Moderate cases are characterized by the anterior and posterior flattening in the inferior cornea. Brunette and associates reported a mild corneal anterior surface deformation and significant central bulging of the posterior surface toward the anterior chamber.<sup>23</sup> We previously reported that corneal guttae are dominant in inferotemporal areas than superionasal areas among peripheral zone.<sup>2</sup> Thus, it was assumed that the asymmetric onset of corneal guttae caused tomographic asymmetry at the posterior surface. Although it is unclear why the anterior inferior surface flattened, it compensated the posterior inferior surface flattening for optical characteristics. Cases with severe corneal edema are complicated with irregularity in the anterior and posterior surfaces of the cornea. In addition to the morphologic change of moderate cases, they are often characterized by folds in the Descemet membrane and epithelial edema. It was thought that these changes resulted in a higher amount of higher-order irregularity component in severe cases.

Better CDVA was significantly associated with a steeper spherical component, and smaller amounts of asymmetry in the anterior corneal surface. Better CDVA was associated with a steeper spherical component, a smaller amount of asymmetry, and a higher-order irregularity component in the posterior corneal surface. Although spherical components in the anterior and posterior cornea can be corrected during CDVA measurements, they were significantly



associated with CDVA. The conflict can be due to some confounding factors such as the scattering. Although CDVA was significantly correlated with asymmetry components in both the anterior and posterior surfaces, it was significantly associated with higher-order irregularity of only the posterior surface, not the anterior surface. It can be an asymmetric onset of higher-order irregularity in the anterior and posterior corneal surfaces.

In conclusion, we demonstrated that patients with severe FECD had a higher asymmetry and higher-order irregularity components in the anterior and posterior surface of the cornea and a flatter spherical component in the posterior surface of the cornea using Fourier analysis. This analysis enabled us to understand tomographic and optical change of the cornea with FECD progression.

FUNDING/SUPPORT: THIS WORK WAS SUPPORTED BY MHLW RESEARCH, JAPAN ON RARE AND INTRACTABLE DISEASES PROGRAM Grant Number 20FC1032.

Financial Disclosure: YO reports personal fees from Japanese Tissue Engineering, Alcon, United States, Santen, Japan, Otsuka, IQVIA, and Senju outside of the submitted work. YY reports personal fees from Santen and Alcon outside the submitted work. SK reports grants from SEED, Japan, Shire Takeda, and Johnson & Johnson, United States and personal fees from Alcon, Menicon, Oculus, Otsuka, and Santen outside the submitted work. RK reports grants from Topcon, Senju, Pfizer, and Novartis and personal fees from Topcon, Bayer, Roche, Takeda, Kowa Pharmaceutical, NovoNordisk, Astellas, Santen, and Nitto medic outside the submitted work. NM reports grants from Topcon during the conduct of the study and personal fees from Alcon, Bausch & Lomb, HOYA, Johnson & Johnson, Otsuka, Santen, Senju, Tomey, Menicon, Pfizer, and Santec outside the submitted work. KN reports personal fees from Japanese Tissue Engineering, Carl Zeiss, Alcon, Otsuka, Santen, Senju, and Wakamoto outside the submitted work.

All authors attest that they meet the current ICMJE criteria for authorship.

## REFERENCES

1. Weiss JS, Moller HU, Aldave AJ, et al. IC3D classification of corneal dystrophies—edition 2. *Cornea* 2015;34(2):117–159.
2. Fujimoto H, Maeda N, Soma T, et al. Quantitative regional differences in corneal endothelial abnormalities in the central and peripheral zones in Fuchs' endothelial corneal dystrophy. *Invest Ophthalmol Vis Sci* 2014;55(8):5090–5098.
3. van den Berg TJ. Importance of pathological intraocular light scatter for visual disability. *Doc Ophthalmol* 1986;61(3-4):327–333.
4. Watanabe S, Oie Y, Fujimoto H, et al. Relationship between corneal guttae and quality of vision in patients with mild fuchs' endothelial corneal dystrophy. *Ophthalmology* 2015;122(10):2103–2109.
5. Ang M, Baskaran M, Werkmeister RM, et al. Anterior segment optical coherence tomography. *Prog Retin Eye Res* 2018;66:132–156.
6. Maeda N. Optical coherence tomography for corneal diseases. *Eye Contact Lens* 2010;36(5):254–259.
7. Kiritoshi S, Oie Y, Nampei K, et al. Anterior segment optical coherence tomography angiography in patients following cultivated oral mucosal epithelial transplantation. *Am J Ophthalmol* 2019;208:242–250.
8. Yasuno Y, Madjarova VD, Makita S, et al. Three-dimensional and high-speed swept-source optical coherence tomography for in vivo investigation of human anterior eye segments. *Opt Express* 2005;13(26):10652–10664.
9. Hjortdal JO, Erdmann L, Bek T. Fourier analysis of videokeratographic data. A tool for separation of spherical, regular astigmatic and irregular astigmatic corneal power components. *Ophthalmic Physiol Opt* 1995;15(3):171–185.
10. Olsen T, Dam-Johansen M, Bek T, Hjortdal JO. Evaluating surgically induced astigmatism by Fourier analysis of corneal topography data. *J Cataract Refract Surg* 1996;22(3):318–323.
11. Oshika T, Tomidokoro A, Maruo K, et al. Quantitative evaluation of irregular astigmatism by fourier series harmonic analysis of videokeratography data. *Invest Ophthalmol Vis Sci* 1998;39(5):705–709.
12. Raasch TW. Corneal topography and irregular astigmatism. *Optom Vis Sci* 1995;72(11):809–815.
13. Baek TM, Lee KH, Tomidokoro A, Oshika T. Corneal irregular astigmatism after laser in situ keratomileusis for myopia. *Br J Ophthalmol* 2001;85(5):534–536.
14. Oshika T, Tanabe T, Tomidokoro A, Amano S. Progression of keratoconus assessed by fourier analysis of videokeratography data. *Ophthalmology* 2002;109(2):339–342.
15. Tomidokoro A, Oshika T, Kojima T. Corneal astigmatism after scleral buckling surgery assessed by Fourier analysis of videokeratography data. *Cornea* 1998;17(5):517–521.
16. Meadows DN, Eghrari AO, Riazuddin SA, et al. Progression of Fuchs corneal dystrophy in a family linked to the FCD1 locus. *Invest Ophthalmol Vis Sci* 2009;50(12):5662–5666.
17. Krachmer JH, Schnitzer JI, Fratkin J. Cornea pseudoguttata: a clinical and histopathologic description of endothelial cell edema. *Arch Ophthalmol* 1981;99(8):1377–1381.
18. Krachmer JH, Purcell JJ Jr, Young CW, Bucher KD. Corneal endothelial dystrophy. A study of 64 families. *Arch Ophthalmol* 1978;96(11):2036–2039.
19. Louttit MD, Kopplin LJ, Igo RP Jr, et al. A multicenter study to map genes for Fuchs endothelial corneal dystrophy: baseline characteristics and heritability. *Cornea* 2012;31(1):26–35.
20. Chylack LT Jr, Wolfe JK, Singer DM, et al. The lens opacities classification system III. The Longitudinal Study of Cataract Study Group. *Arch Ophthalmol* 1993;111(6):831–836.
21. Wacker K, McLaren JW, Amin SR, et al. Corneal high-order aberrations and backscatter in Fuchs' endothelial corneal dystrophy. *Ophthalmology* 2015;122(8):1645–1652.
22. Wacker K, McLaren JW, Patel SV. Directional posterior corneal profile changes in Fuchs' endothelial corneal dystrophy. *Invest Ophthalmol Vis Sci* 2015;56(10):5904–5911.
23. Brunette I, Sherknies D, Terry MA, et al. 3-D characterization of the corneal shape in Fuchs dystrophy and pseudophakic keratopathy. *Invest Ophthalmol Vis Sci* 2011;52(1):206–214.